Study of the temperature-induced aggregation of polyoxometalate-poly(N,N-diethylacrylamide) hybrids in water

Jennifer Lesage de La Haye, André Pontes da Costa, Gaelle Pembouong, Laurent Ruhlmann, Bernold Hasenknopf, Emmanuel Lacote, Jutta Rieger

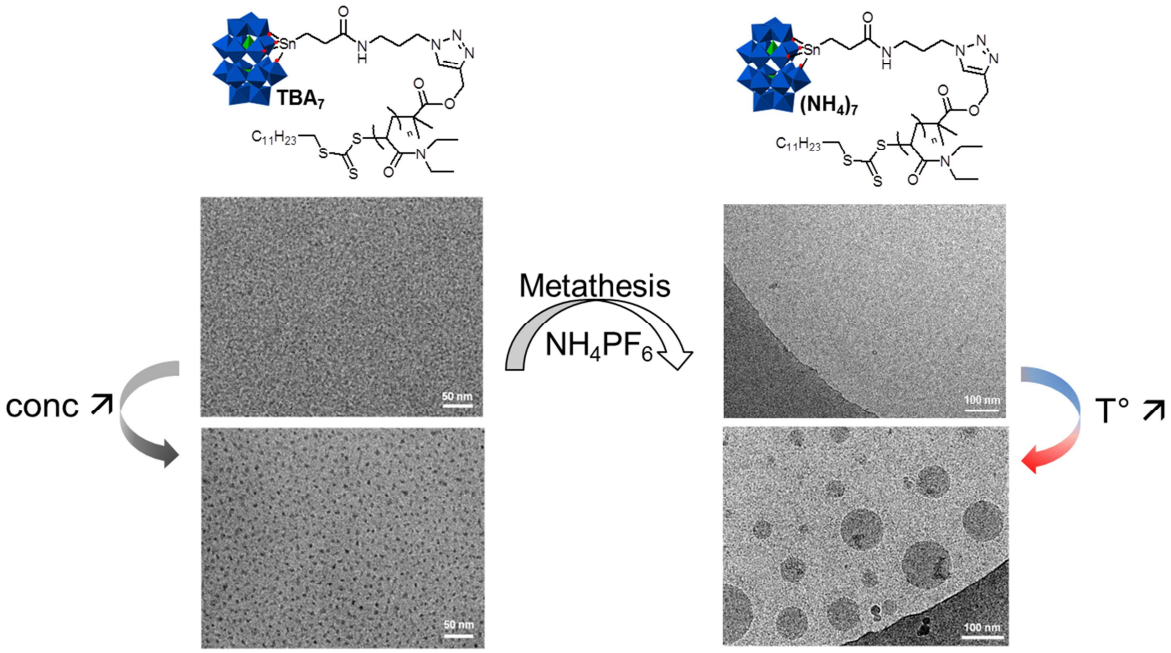

Study of the temperature-induced aggregation of polyoxometalate-poly(*N,N*-diethylacrylamide) hybrids in water

Jennifer Lesage de la Haye,[a,b,c] André Pontes da Costa,[a,b] Gaëlle Pembouong,[a,b] Laurent Ruhlmann,[d] Bernold Hasenknopf,*[a,b] Emmanuel Lacôte,*[c,e] Jutta Rieger*[a,b]

[a] Sorbonne Universités, UPMC Univ Paris 06, UMR 8232, Institut Parisien de Chimie Moléculaire (IPCM), F-75005, Paris, France.

[b] CNRS, UMR 8232, Institut Parisien de Chimie Moléculaire (IPCM), F-75005, Paris, France.

[c] ICSN CNRS, Av. de la Terrasse, 91198 Gif-sur-Yvette Cedex, France.

[d] Université de Strasbourg, Laboratoire d'Electrochimie et de Chimie Physique du Corps Solide, Institut de Chimie, 67081 Strasbourg, France.

[e] Université de Lyon, Institut de chimie de Lyon, UMR 5265 CNRS-Université Lyon I-ESCPE Lyon, 69616 Villeurbanne, France.

Corresponding Authors:

*E-mail: bernold.hasenknopf@upmc.fr, emmanuel.lacote@univ-lyon1.fr, jutta.rieger@upmc.fr

KEYWORDS. Polyoxometalates, RAFT, thermoresponsive, LCST, DSC, cryo-TEM, self-assembly.

ABSTRACT. In this article, we study the temperature-induced phase transition of aqueous solutions of tailor-made Dawson polyoxometalate-poly(*N,N*-diethylacrylamide) hybrids (POM-PDEAAm) by means of differential scanning calorimetry, dynamic light scattering and cryo-TEM microscopy. Generally, the typical thermoresponsive aggregation of the PDEAAm in water was transferred to the hybrids. The organization of the compounds in solution below and above the transition temperature was studied, and precious insights in the aggregation mechanisms were obtained. The impact of the polymer chain-ends, the nature of the counterions of the negatively charged POM subunits and the weight fraction of the POM was elucidated, revealing a strong influence of the POM's counter-ions. Temperature and nature of the cations are thus two external factors that can be used to control the properties of the conjugates.

INTRODUCTION

Polyoxometalates (POMs) are negatively charged metal-oxygen clusters of early transition metals in high oxidation states (most commonly V^V, Mo^{VI} and W^{VI}) which have important electronic and chemical properties making them suited for applications in catalysis and materials science.[1-4] Synthetic methods have been devised to obtain organo-POMs.[5-7] A particular case constitutes polymer-POM hybrids that combine the characteristics of polymers with that of their inorganic counterparts.[8] However, only a limited number of examples of covalently linked POM-polymer conjugates have been reported in the literature,[9,10,11] and even less studies have been dedicated to their physicochemical characterization. Depending of the method used, POM units can be randomly distributed along the polymer backbones or be localized at their chain end. In the latter case, the inorganic and organic subunits are well-separated, making them especially appealing for self-assembly into nanostructured materials.[11c] In view of their potential applications, hybrids systems of which the assembly might be externally tuned seem particularly appealing. [11c,12]

As an example, Wang's group synthesized a POM-polystyrene hybrid composed of a $\{(Bu_4N)_5[H_4P_2W_{15}V_3O_{62}]\}$ Dawson vanado-tungstate head and a polystyrene (PS) tail *via* ATRP (atom transfer radical polymerization).[13] The proton salts of the obtained POM-PS composite formed aggregates in DMF, which showed a transition from vesicles to tubular structures upon thermal annealing, these latter being thermodynamically more stable.[14] To the best of our knowledge very few stimuli-responsive covalent POM-polymer hybrids have been studied so far.[12,15]

We had reported previously[11e] the synthesis of an α_2-substitued Dawson phosphotungstate grafted by a poly(*N*,*N*-diethylacrylamide) (PDEAAm) oligomer $[\alpha_2\text{-}P_2W_{17}O_{61}SnCH_2CH_2C(=O)NHCH_2\text{-poly}(N,N\text{-diethylacrylamide})]^{7-}$, where the molar mass of the short polymer chain was in the same range as that of the inorganic cluster (about 5 kg mol^{-1}). Subsequently we reported the preparation of a series of water-soluble POM-PDEAAm hybrids via RAFT polymerization and demonstrated their catalytic activity imparted by the α_1-substituted Dawson phosphotungstate $[\alpha_1\text{-}P_2W_{17}O_{61}\{Sn(CH_2)_2C(O)NH(CH_2)_3R\}]$.[16] In both cases, poly(*N*,*N*-diethylacrylamide) (PDEAAm) had been selected as the polymer component for its

temperature-dependent solubility in water,[17,18] a feature that characterizes it as smart material. Upon heating PDEAAm solutions above its transition temperature (TT), phase separation occurs and the polymer chains may form colloidally stable aggregates, called mesoglobules.[18] This feature results from the temperature dependency of hydrogen bonds and hydrophobic interactions, and viscoelastic effects.

We study herein in detail this thermally-induced phase transition of our α_1-substituted Dawson phosphotungstate-PDEAAm hybrids by means of differential scanning calorimetry (DSC), dynamic light scattering (DLS) and cryo-TEM (Scheme 1), and discuss the impact of polymer molar mass, solution concentration and counterions associated to the POM on the transition.

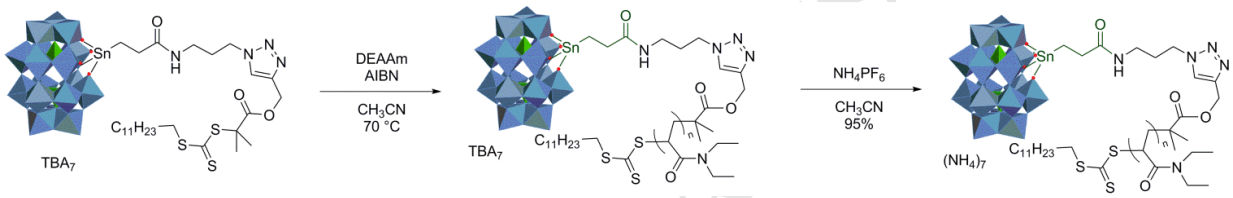

Scheme 1. Synthesis pathway towards POM-PDEAAm hybrids.[16]

EXPERIMENTAL SECTION

Materials. PDEAAm (PX) and POM-PDEAAm hybrid, tetrabutylammonium (TBA) salts, (PPX-T) samples were synthesized as reported before.[16] The molar mass of the hydrophobic POM-TBA salt is $MW_{\text{POM-TTC-T, TBA}}$ = 6537 g mol^{-1} and that of the hydrophilic NH_4^+ one is $MW_{\text{POM-TTC-N, NH4}}$ = 4966 g mol^{-1}.

Ion Exchange: Synthesis of $(NH_4)_7[\alpha_1$-POM]-PDEAAm (6). In a typical example, a solution of NH_4PF_6 (3.57×10^{-5} mol, 20 equiv, 6 mg) in acetonitrile (1 mL), which had been filtered on cotton before use, was added to a solution of hybrid PP55-T (1.78×10^{-6} mol, 1 equiv, 100 mg) in acetonitrile (3 mL) under nitrogen atmosphere. The solution was concentrated *in vacuo* and redissolved in a minimum of acetonitrile. It was then precipitated upon addition of Et_2O, and the solid was isolated by centrifugation. This process was repeated three times. The solid was washed with pure Et_2O and dried *in vacuo* to obtain a white solid (91.8 mg, 95% yield). It should

be noted, that the final product contained still important amounts of NH_4PF_6. Its quantity was estimated by ^{31}P NMR to 44 equivalents relative to the POM unit. ^{31}P NMR (121.5 MHz, CD_3CN): δ –143.2 (sept, PF_6^-), δ –11.9 (s, 1 P, PW_9), –6.5 (s+d, 1 P, J_{SnP} = 41.5 Hz, PW_8Sn).

Removal of the thiocarbonylthio end group from PDEAAm-C_{12}: synthesis of P55-H.[11e] 150.0 mg of PDEAAm-C_{12} (M_n = 47.3 kg mol^{-1}, M_w/M_n = 1.18, 0.003 mmol, 1.0 eq.) was dissolved in 1 mL propan-2-ol and heated under reflux to 80 °C. A solution of lauroyl peroxide (1.6 mg, 0.004 mmol, 1.3 eq.) in propan-2-ol (0.4 mL) and toluene (0.1 mL) was added in seven portions every 3 h under a nitrogen atmosphere. The reaction mixture was then precipitated in cold pentane (88.6 mg, 59%, $M_{n,LS}$ (SEC) = 47.0 kg mol^{-1}, M_w/M_n (PMMA) = 1.18).

Instrumentation.

Differential Scanning nanoCalorimetry (nanoDSC). Calorimetric measurements were done with a N-DSC III instrument from Calorimetry Sciences Corporation at a scan rate of 0.5 °C min^{-1}. The system consists of two capillary cells, respectively reference and sample, of 0.3 mL under pressure 5×10^5 Pa. Samples of a concentration of 5 mg mL^{-1} were prepared and stirred during one day before analysis. All samples were degassed under reduced pressure before injection and were not capped. They were equilibrated for 10 min before each heating and cooling run, going from 5 °C to 85 °C. First, a baseline scan (water in both the reference and the sample cells) was recorded in identical conditions and subtracted from the sample scan. The transition temperature was determined at the onset of the transition, T_{onset}, *i.e.* the intersection of the baseline and the leading edge of the endotherm, and the transition enthalpy (ΔH) of the polymers was calculated by integrating endotherms at the second heating run (see Figure SI-1).[19] The error on the enthalpy of the endotherms was estimated to be in the range of 5%.

Dynamic Light Scattering. Dynamic light scattering (DLS) measurements were carried out using a Zetasizer Nano S90 from Malvern using a 5 mW He-Ne laser at 633 nm at 20 °C and 70 °C. The samples' concentration was generally 5 mg mL^{-1}, i.e. the same used for the determination of calorimetric measurements with nanoDSC. To investigate the influence of the concentration, some samples were studied at different concentrations: at 1 mg mL^{-1}, 5 mg mL^{-1} and 10 mg mL^{-1}. The solutions were dissolved and stirred during one day before analysis. Results were obtained in duplicate.

Cryo-TEM. Cryo-Transmission Electron Microscopy (cryo-TEM) was used to determine the shape and size of the POM-polymer hybrids. Two types of cryo-TEM analyses were performed: To analyze solutions below the transition temperature (TT) of PDEAAm, 4 µL of an aqueous solution of POM-polymer (5 mg mL^{-1}) was deposited at room temperature on a quantifoil grid and rapidly frozen in liquid ethane. In the second case, the aqueous POM-polymer solution was heated until it became turbid, rapidly deposited on a quantifoil grid and then rapidly frozen in liquid ethane. The grids were transferred and observed at -180 °C on a JEOL JEM-2100 LaB6 microscope operating at 200 kV under low-dose conditions (less than 10 electrons $Å^{-2}$ s^{-1}) at a nominal magnification of 20 000 and 40 000. Images were recorded on a 2k by 2k pixels CCD camera (Gatan Ultrascan 1000).

Size Exclusion Chromatography (SEC). Size exclusion chromatography measurements were performed with a Viscotek Tetra Detector Array (TDA) including a differential refractive index detector (RI), a right (90°) and a low (7°) angle light scattering (LS) detector (RALS/LALS), a four-capillary differential viscometer, and a diode array UV detector. DMF (+ LiBr, 1 g L^{-1}) was used as the mobile phase at a flow rate of 0.8 mL min^{-1} and toluene served as a flow rate marker. All polymers were injected at a concentration between 3.5 mg mL^{-1} and 7 mg mL^{-1} after filtration through a 0.20 µm pore-size membrane. The separation was carried out on two PSS GRAM 1000 Å columns (8 × 300 mm; separation limits: 1 to 1000 kg mol^{-1}) and one PSS GRAM 30 Å (8 × 300 mm; separation limits: 0.1 to 10 kg mol^{-1}). Columns and detectors were maintained at 60 °C. The OmniSEC 4.6 software was used for data acquisition and data analysis. The molar mass distributions (dispersity $Đ = M_w/M_n$) were derived from the RI signal by a calibration curve based on PMMA standards (Polymer Standards Service). The number-average molar masses, $M_{n,LS}$, were calculated using the RALS/LALS, RI and viscosity signals. The refractive index increment (*dn/dc*) of POM-PDEAAm PP55-T was measured with the online RI detector by injecting solutions (in DMF + 1 g L^{-1} LiBr) at three concentrations (c_1 = 3.5 mg mL^{-1}, c_2 = 5 mg mL^{-1} and c_3 = 6 mg mL^{-1}). The *dn/dc* was calculated by plotting the RI area (integrated from the RI signal) versus the injected concentration with the OmniSEC software. Because the RI area is assumed to be proportional to the refractive index of the sample, the *dn/dc* can be calculated from the slope of the straight line. The refractive index increment (*dn/dc* = ν) for the POM-TTC ν_x was calculated according to $\nu = w_x\nu_x + w_y\nu_y$, where ν is the refractive index increment of the hybrid, w_x is the weight fraction of POM-TTC, w_y is the weight fraction of

PDEAAm and v_y = 0.073 mL g^{-1} for PDEAAm. A value of v_x = 0.062 mL g^{-1} was obtained for POM-TTC.

RESULTS

Table 1. Characteristics of poly(*N,N*-diethylacrylamide) samples

PDEAAm-C_{12} [a]	TTC-C_{12} fraction / wt%	$M_{n,LS}$ [b] / kg mol^{-1}	M_w/M_n [c]
P30	0.9	29.4	1.4
P55	0.5	52.9	1.3
P90	0.3	88.6 *(57.8[d])*	1.3
P55-H	-	47.7	1.2
P90-H	-	*(56.0[d])*	1.3

[a] « P30 » stands for PDEAAm-C_{12} with M_n close to 30 kg mol^{-1}; P55-H refers to PDEAAm-H, obtained after removal of the TTC-alkyl chain (see SI). [b] Number-average molar mass (M_n) determined by SEC in DMF (+LiBr) with light scattering (LS). [c] M_w/M_n determined by SEC in DMF (+LiBr) with PMMA calibration, [d] M_n determined SEC in DMF (+LiBr) with PMMA calibration.

Table 2. Characteristics of POM-poly(*N,N*-diethylacrylamide) hybrids.

POM-PDEAAm-C_{12} [a]	POM fraction/ wt%	$M_{n,LS}$ [b]/ kg mol^{-1}	M_w/M_n [c]
PP15-T	29	14.7	1.1
PP30-T	14	30.8	1.2
PP55-T	8	56.1	1.3
PP100-T	4	97.9	1.5

[a] « PP30-T » stands for POM-polymer with M_n close to 30 kg mol^{-1} and tetrabutylammonium ion (T) as counterion for the POM. [b] Number-average molar mass (M_n) determined by SEC in DMF (+LiBr) with light scattering (LS). [c] M_w/M_n determined by SEC in DMF (+LiBr) with PMMA calibration.

A series of well-defined PDEAAm and POM-PDEAAm hybrids was synthesized according to our previous report[16] by reversible-addition fragmentation chain transfer (RAFT) polymerizations with polymer segments of different molar masses. In addition, we also prepared the POM-PDEAAm hybrids with different counterions. It should be noted that the selected synthesis pathway (Scheme 1) provides polymers whose chains are terminated by a hydrophobic dodecyl chain (C_{12}). POM-polymer hybrids were named PPXX-Y, where PP designates the POM-polymer hybrid (in contrast to P for the pure polymer, see below), XX indicates the range of M_n of the hybrids in kg mol^{-1} and Y indicates the counterion (T for tetrabutylammonium (TBA) and N for ammonium (NH_4^+)). Thus, for example PP30-T stands for a POM-polymer conjugate with M_n close to 30 kg mol^{-1} and tetrabutylammonium ion as counterion of the POM.

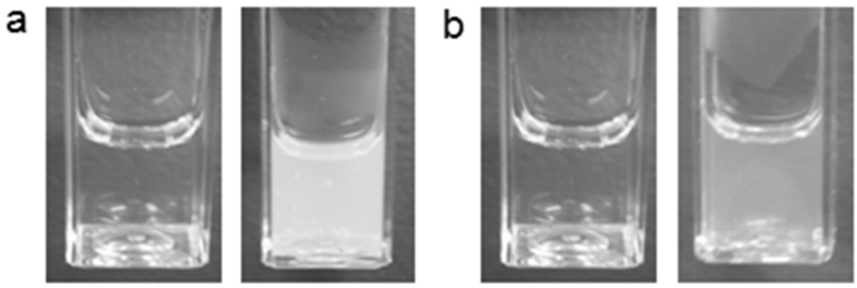

Figure 1. Photographs of aqueous solutions (5 mg mL^{-1}) of (a) PP55-T at 20 °C (left) and 70 °C (right), and (b) PP55-N at 20 °C (left) and 70 °C (right).

Calorimetric Phase Transition Analyses. We observed that aqueous solutions of the POM-PDEAAm hybrids (both the TBA and the NH_4^+ salts) turned cloudy or whitish upon heating, indicating that the hybrids exhibit, like PDEAAm, a temperature-dependent solubility in water (Figure 1). This macroscopically visible phase separation is an endothermic process since energy is needed for disrupting hydrogen bonds between water molecules and the polymer. It can be monitored and quantified by ultrasensitive nanoDSC, which measures changes of the partial heat capacity (C_p) of a solution as a function of the temperature. The transition temperatures (TT) of the compounds can be measured at the onset of the DSC transition endotherms (T_{onset}) and the transition enthalpies (ΔH) can be calculated from the area under the endotherms (see Figure

SI-1).[19] We therefore used nanoDSC to analyze aqueous solutions of polymers and the corresponding POM hydrids, in order to identify the influence of the molar mass of the polymer, the presence or not of the POM unit and the type of the POM counterion.

Thermal characterization of PDEAAm-C_{12} samples, (P30, P55 and P90), and PDEAAm-H (P55-H, P90-H). The heat-induced transitions of polymer samples PDEAAm-C_{12}, *i.e.* poly(*N,N*-diethylacrylamide) terminated by a dodecyl alkyl chain and PDEAAm without any dodecyl alkyl chain, were investigated first. Actually, an impact of terminal alkyl chains on the temperature-induced dehydration has already been reported for other polymers,[20,21] but - to the best of our knowledge - alkyl chain end-capped-PDEAAms have never been studied by DSC or DLS. This first study aims thus at establishing a proper reference.

As already observed in the literature for PDEAAm samples obtained by non-controlled radical polymerization, the thermograms were endothermic, broad and asymmetric or even bimodal with a sharp increase of the heat capacity at the low temperature side followed by a more gradual decrease of the heat capacity (Figure 2).[18,22,23] Independently of the molar mass, all PDEAAm-C_{12} samples showed a TT of about 30 °C, determined at the onset of the transition (Table 3 and Figure SI-1). In addition, the transition enthalpy ΔH (in kJ $mol_{polymer}^{-1}$) increased as expected with increasing molar mass of PDEAAm (P30 to P90), *i.e.* with increasing number of monomer units (Table 3). The molar transition enthalpy ΔH per monomer unit (DEAAm) was similar for all compounds, in the range of 6.5 to 7 kJ mol_{DEAAm}^{-1}, *i.e.* close to values reported in the literature.[22,24]

Moreover, PDEAAm whose TTC-C_{12} end chain had been removed, PDEAAm-H samples P55-H and P90-H (Figure SI-2) were also analyzed. The transitions were again broad and the onsets of the transitions were determined to be 33°C and 29°C for P55-H and P90-H respectively. For both compounds, the measured enthalpy per monomer unit was slightly higher than for the dodecyl-end-capped polymers, in the range of 7 kJ mol_{DEAAm}^{-1}. (Table 3)

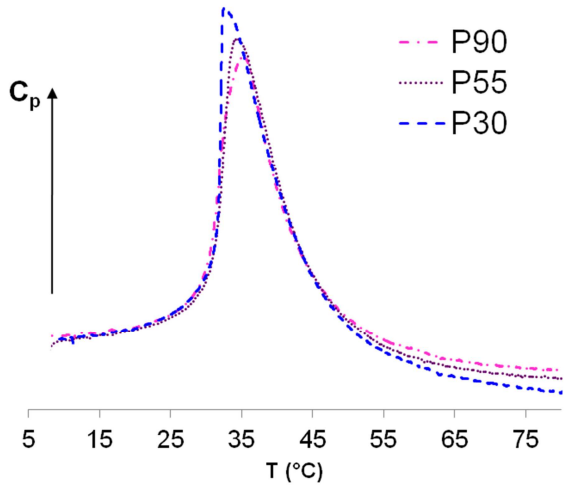

Figure 2. Temperature dependence of specific heat capacity (C_p in kJ mol_{DEAAm}^{-1} K^{-1}) of PDEAAm-C_{12} aqueous solutions (5 mg mL^{-1}).

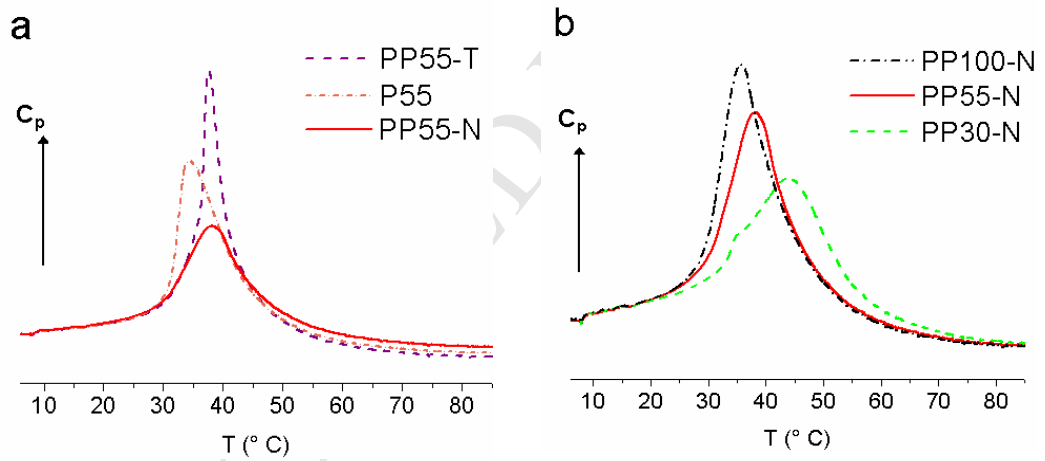

Figure 3. Temperature dependence of specific heat capacity (C_p in kJ mol_{DEAAm}^{-1} K^{-1}) of POM-PDEAAm hybrids' and PDEAAm-C_{12} aqueous solutions (5 mg mL^{-1}).

Thermal study of the POM-PDEAAm Hybrids. In Figure 3a, the endotherms for the ammonium and TBA salts of POM-PDEAAm hybrids (PP55-N and PP55-T) were overlaid with those of the corresponding polymer P55. The onset of the temperature transition was similar for

all compounds, but the temperature at the maximum of the transition was significantly higher for the hybrids. In addition, the full width at half maximum of the endotherm was the smallest for TBA salt hybrid PP55-T, with a transition enthalpy very close to that determined for polymer P55 (6.5 and 6.6 kJ mol_{DEAAm}^{-1} respectively).

For the ammonium salt PP55-N the full width at half maximum of the endotherm was the largest and the measured enthalpy was significantly lower than for P55 and PP55-T (4.5 kJ mol_{DEAAm}^{-1} against 6.6 and 6.5 kJ mol_{DEAAm}^{-1}). When the molar mass of the PDEAAm segment was decreased, *i.e*. when the proportion of POM was increased, the endotherm was even larger (Figure 3b) and the molar enthalpy per monomer unit further decreased (Table 3). This stands in contrast to the pure polymer PDEAAm-C_{12} series and clearly shows that the $(NH_4)_7$ POM subunit has a strong impact.

Furthermore, a little shoulder at the beginning of the transition was observed for the lowest molar mass hybrid PP30-N. Such a gradual, broad transition along with the presence of a shoulder has formerly been attributed to the presence of salts.[25,26] Because an excess of NH_4PF_6 was used in the synthesis of the NH_4^+, some salt remained in the samples. However, when equivalent quantities of NH_4PF_6 were added to polymer sample PDEAAm-C_{12} P55 no change of either the T_{onset} or the width at half maximum was observed (Figure SI-3). However, the presence of the salt accentuated the bimodal character of the transition with an increased enthalpy of the first step of the transition (see both transitions at 33 and 36 °C in Figure SI-3, Table 3). The broadening of the transition and the decrease in enthalpy observed for the hybrids should thus be attributed to the presence of the POM segment (see discussion below).

The transition was globally reversible since the thermograms for the heating and cooling process were roughly inverted copies with almost equal ΔH (see PP55-N as example in Figure SI-4).

Table 3. Transition temperatures and transition enthalpies of PDEAAm and POM-PDEAAm hybrids determined by nanoDSC.

Sample type	Sample name	TT (°C)	ΔH (MJ $mol_{polymer}^{-1}$)	ΔH (kJ mol_{DEAAm}^{-1})
PDEAAm	P30	30	1.6	6.9
	P55	30	2.7	6.6
	P90	30	4.5	6.5
	P55-H	33	2.7	7.4
	P90-H	29	5.2	7.6
	P55+NH_4PF_6	30	2.9	7.1
POM-PDEAAm (NH_4^+ salts)	PP30-N	30	0.6	3.2
	PP55-N	29	1.7	4.5
	PP100-N	28	3.9	5.4
POM-PDEAAm (TBA salt)	PP55-T	31	2.5	6.5

Dynamic light scattering and cryo-transmission electron microscopy study.

As shown above, DSC measurements of aqueous hybrid solutions revealed a typical temperature-induced transition originating from the covalently linked PDEAAm segment. The consequence of this change in chain conformation is the formation of light scattering aggregates that can be detected by the naked eye (Figure 1) and characterized more deeply by light scattering techniques or electron microscopy. Aqueous solutions of PDEAAm, PDEAAm-C_{12} and POM-polymer hybrids far below and beyond the TT were therefore studied by dynamic light scattering (DLS) and cryo-transmission electron microscopy (cryo-TEM).

DLS of all aqueous solutions of the polymers PDEAAm-C_{12} and the hybrids (TBA and NH_4^+ salts) at 20 °C showed low scattering intensities consistent with the presence of small unimers (determined to be about 10 nm in diameter, Table SI-1, Figure SI-5 and SI-7) and some swollen aggregates of larger size. Those aggregates were not observed in the number-weighted mode

(Figure SI-5c and SI-7c,d; number mode), but they were clearly detected in the intensity-weighted mode (Figure SI-5a and SI-7 a,b). It should be noted that the intensity mode exaggerates the proportion of large scattering aggregates as the scattering intensity is strongly dependent on the particle diameter.[27] Interestingly, those aggregates were reformed after filtration through 0.2 µm membrane, which indicates that they were not artifacts like dust but that they do exist, in equilibrium with the unimers. For all compounds, the polymer PDEAAm-C_{12} and the hybrids, the size of the unimers was found to increase slightly with increasing molar mass of the polymer (Table SI-1).

In contrast to these results, aqueous solution of PDEAAm-H compound P55-H without a dodecyl chain, showed one size distribution with a z-average diameter of around 100 nm. No unimers were detected (Table SI-1, Figure SI-6).

When heated to 70 °C, *i.e.* beyond the transition temperature range, PDEAAms and hybrids samples showed increased scattering intensities consistent with the formation of light scattering particles. P55-H was the only sample where the temperature-induced aggregates were smaller than below TT (example, D_z = 118 nm at 20 °C and D_z = 31 nm at 70 °C for P55-H, Figure SI-6, Table 4). Only after repeated and prolonged heating times, larger aggregates were also detected. For all other samples, in both the intensity and number mode, one single size distribution was reproducibly detected with a z-average diameter between 40 and 110 nm. In more detail, the z-average diameter of the aggregates formed by the NH_4^+ hybrids was between 40-50 nm and as such very similar to that of PDEAAm-C_{12} aggregates (Table 4, Figure 4a and Figure SI-5b). For both types of samples no significant trend in D_z with polymer chain length was observed. In contrast, for the TBA salts, larger aggregates were observed, whose D_z increased with decreasing chain length of the polymer (Table 4 and Figure 4b).

Table 4. D_z-average diameter of aggregates formed in aqueous solutions (5 mg mL^{-1}) of PDEAAm-C_{12}, PDEAAm-H and POM-polymer hybrids (TBA and NH_4^+ salts) at 70 °C.

conc. (mg mL^{-1})	z-average diameter (D_z, nm)											
	PDEAAm-H		PDEAAm-C_{12}			POM-PDEAAm (NH_4^+ salt)			POM-PDEAAm (TBA salt)			
	P55-H	P90-H	P30	P55	P90	PP30-N	PP55-N	PP100-N	PP15-T	PP30-T	PP55-T	PP100-T
1	185	177	-	48	-	47	45	-	-	-	48	-
5	31*	20	41	38	46	39	46	44	(90)**	110	65	55
10	9*	-	-	30	-	-	43	-	-	-	84	-

* Larger aggregates were formed when heated for a prolonged period of time (> 3 h); **polydisperse sample.

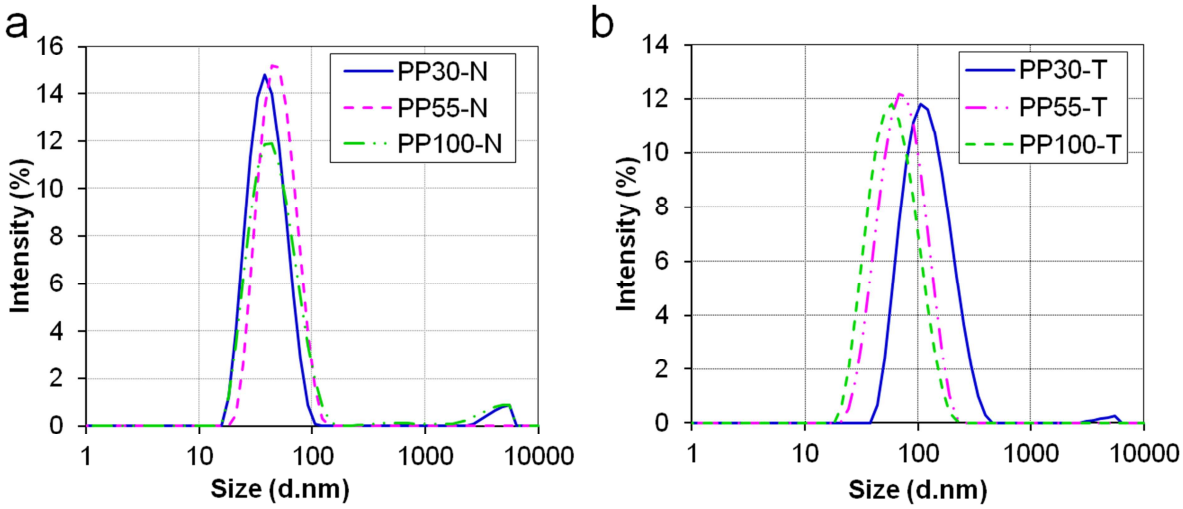

Figure 4. Intensity-weighted hydrodynamic diameter distributions for aqueous solutions (5 mg mL^{-1}) of hybrids, (a) NH_4^+ salt and (b) TBA salt at 70 °C.

For hybrid PP100-T (possessing the longest polymer chain, *i.e.* the smallest proportion of POM, ~4 wt%), a diameter close to that of the pure polymer samples was determined (55 nm), whereas the lower molar mass hybrid PP30-T (14 wt% POM) formed aggregates twice the size (110 nm). Further increase of the proportion of POM to 29 wt% (PP15-T, Figure SI-8b) led to a marked broadening of the size distribution (Table 4). As with the PDEAAm-C_{12} series, for all hybrids (except PP15-T) the temperature-induced aggregation was reversible, *i.e.* the size of the aggregates formed at 70 °C was always the same after one, two, three or four heating-cooling cycles.

It should be mentioned that in some of the DLS Figures, displayed in intensity, aggregates of very large dimensions (diameters larger than 10 μm) were detected (see for instance Figure 4a, compounds PP30-N and PP100-N). Larger aggregates scatter much more intensively light, and the actual number of the bigger "particles" might thus be considered as very small. We actually did not filter our aqueous solutions and used pristine solutions to perform DLS measurements, in order to avoid any misinterpretation of the results. The large sizes, observed in little quantity, might thus be both, polluting dust or large aggregates formed upon heating.

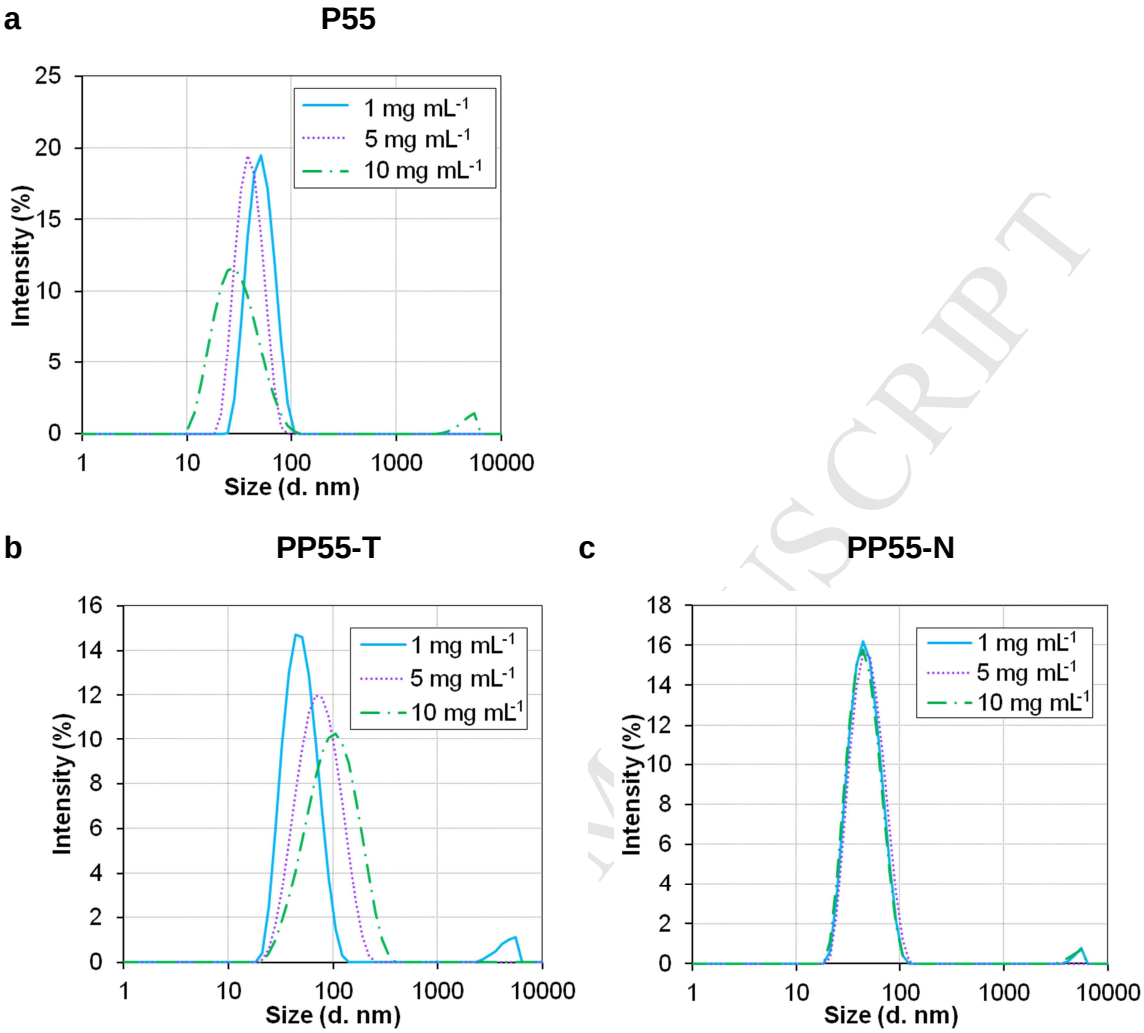

Figure 5. Intensity-weighted hydrodynamic diameter distributions for aqueous solutions of (a) PDEAAm-C_{12} P55, POM-polymer hybrids, (b) TBA salt PP55-T and (c) NH_4^+ salt PP55-N at different concentrations at 70°C.

The preceding DLS measurements were performed in standard conditions at 5 mg mL^{-1}.[28] The thermally-induced aggregation of PDEAAm chains due to a coil-to-globule transition is a kinetically driven process, and depends not only on heating/cooling kinetics but also on the polymer concentration. As summarized in Table 4, DLS measurements at 70°C at different concentrations (1, 5 and 10 mg mL^{-1}) were performed for polymer P55 and the corresponding hybrids, PP55-T and PP55-N. For PDEAAm-C_{12} P55, apparently smaller z-average diameters

and a much larger size distribution were observed with increasing polymer concentration (Figure 5a). Similarly, for TBA hybrid PP55-T the size distribution grew larger, but here the z-average diameter increased (Figure 5b). In contrast, no significant effect of the concentration on either the D_z (40-50 nm) or the size distribution was observed for NH_4^+ salt hybrid PP55-N (Figure 5c). Similar results were obtained for the lower molar mass compound PP30-N (Table 4).

Finally, we also analyzed hybrids solutions by cryo-TEM (C = 5 mg mL^{-1}; Figure 6a and 7a).[29] At 20°C, for both the TBA and ammonium salts only tiny dark spots (1.5-2 nm) attributed to the POM segments and no larger aggregates were observed (Figure 6a and 7a). We were not surprised not to detect any polymer, as PDEAAm is highly hydrated at room temperature and not compact enough to give sufficient contrast with the surrounding water. Interestingly, for the TBA hybrid, at very high concentration (50 mg mL^{-1}) the diameter of the dark spots increased from 1-2 nm to close to 5 nm. These spots seem quite regularly separated from each other, indicating the formation of micellar aggregates, with the hydrophobic TBA-POMs in the core surrounded by the stabilizing polymer chains.

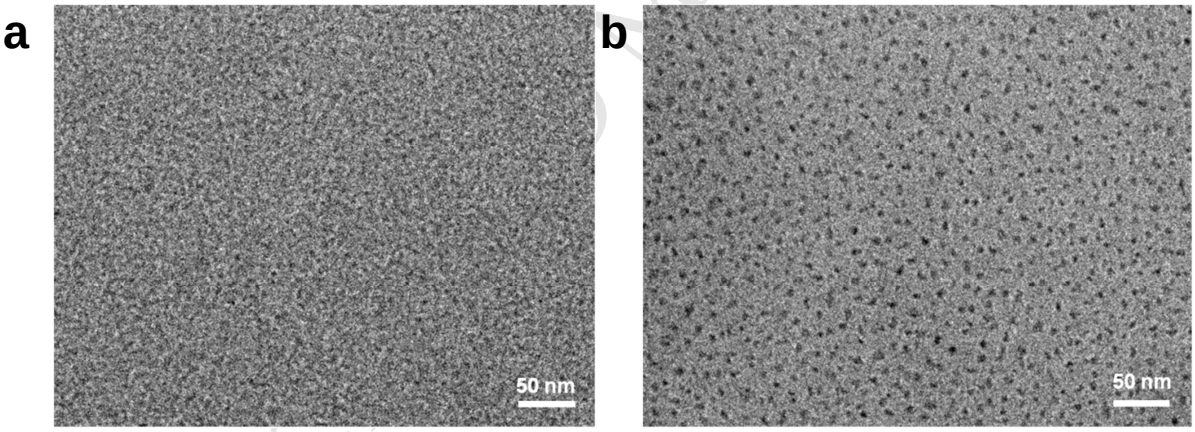

Figure 6. Cryo-TEM images of an aqueous solution of PP55-T fast-frozen from 20 °C (a) at 5 mg mL^{-1} and (b) 50 mg mL^{-1}.

At 70°C, i.e. far above the TT, a large size distribution of spherical particles around 50 nm was observed (Figure 7b). This diameter is comparable to the one determined by DLS, where the sample was however more homogeneous in size. It should be emphasized that cryo-TEM analyses on samples prepared at 70°C are not easy to perform due to the rapidity of the

temperature transition compared to the time necessary to set up and freeze the sample. This might explain the heterogeneity in size observed (diameters ranged from 10 to 100 nm), *i.e.* smaller aggregates could originate from larger aggregates by dissociation upon cooling.

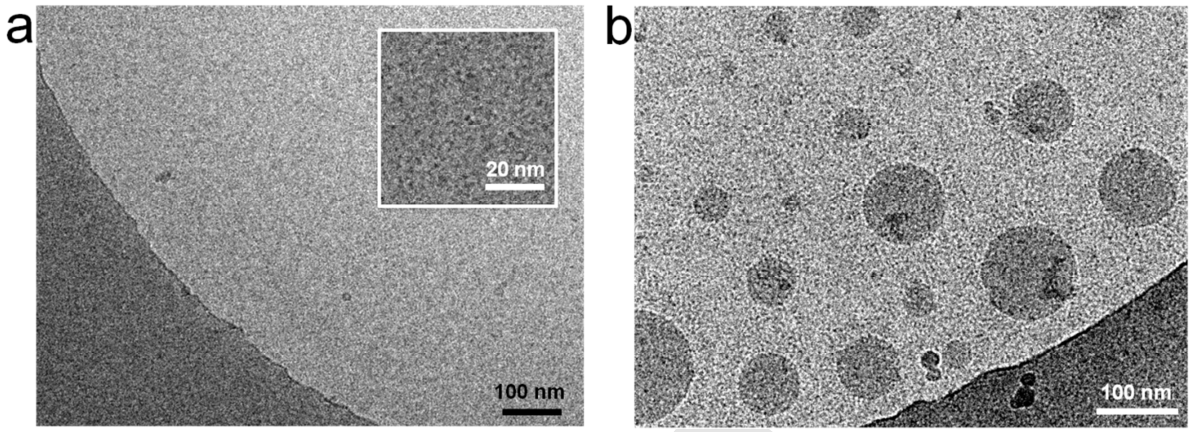

Figure 7. Cryo-TEM images of an aqueous solution of PP55-N (5 mg mL^{-1}) fast-frozen from (a) 20 °C (zoom in inset) and from (b) 70 °C.

DISCUSSION.

N-Substituted poly(acrylamides), particularly poly(*N*-isopropylacrylamide) (PNiPAAm)[30,31] and poly(*N*,*N*-diethylacrylamide),[18,22,32,33] are known to undergo intra- and interchain aggregation upon heating.[34] This thermally induced phase transition occurs with a rearrangement of water molecules and a gain in their entropy, while the polymer structure changes from an extended coil to a collapsed globule conformation. In the case of PDEAAm, which lacks the possibility to form intra- and inter-chain hydrogen bonds due to the secondary amide group, IR measurements have demonstrated that at temperatures below the TT, the amides' carbonyl groups are associated with 0, 1 or 2 water molecules through hydrogen bonds. Upon heating dehydration occurs principally for the amide carbonyl groups that are associated with two water molecules.[22,33] Above the TT most of the amide carbonyl groups are then hydrated with one water molecule, whereas the ethyl groups become fully dehydrated.[35] This only partial dehydration above TT allows to stabilize the aggregates at high temperature (named mesoglobules), avoiding their macroscopic precipitation.

For PDEAAm samples, the asymmetric/bimodal shape of the thermograms that we observed by nanoDSC has already been reported. It was attributed to a two-stage transition, with a first stage where principally intrachain contraction occurs, followed by a second stage where interchain associations become dominant.[18,22,32,33] It had further been demonstrated that the TT and the enthalpy of demixing may vary with the scan rate.[22,32] However and in contrast to poly(*N*,*N*-isopropylacrylamide), the transition of PDEAAm may be reversible and may present no hysteresis if the transition kinetics are respected and heating and cooling are sufficiently slow. Therefore, in this study a low scanning rate of 0.5 °C min^{-1} was chosen.[22] In these conditions, the measured transition temperatures and the enthalpies of the transition of the polymers PDEAAm-C_{12} were in the expected range (literature reports TT of about 30-33 °C[22,24,32,36] and ΔH = 5.7 - 6 kJ $mol_{monomer}^{-1}$ [22,24]). A dependence of the transition temperature on the molar mass of PDEAAm has also been reported,[24,34,36] but in the studied molar mass range (30 to 90 kg mol^{-1}) no significant change of the onset of the transition was observed.

Compared to the H-terminated polymer, we observed that the addition of a hydrophobic trithiocarbonate dodecyl alkyl end group might diminish slightly the TT. Comparing compounds P55-H and P55 the onset of the transition decreased from 33°C to 30 °C. Such a decrease of TT due to the presence of terminal hydrophobic groups is consistent with reports in the literature on (semi)telechelic PNiPAAm or poly(2-alkyl-2-oxazolines).[20,21] The modest decrease in temperature observed in our study should be attributed to the relatively high molar mass of the polymer and the low proportion of the hydrophobic end-group. This decrease in temperature was actually not observed for the higher molar mass compound P90 and P90-H, possibly because the effect of the alkyl chain fades with increasing molar mass (the mass proportion of the C_{12} was only 0.3 wt% in this sample, Table 1).

DLS measurements corroborate these results and indicated a difference in conformation of alkyl-end-capped and H-terminated derivatives at both low and high temperature. They confirm an impact of the C_{12} hydrophobic end chain (see discussion below).

The onset of the transition temperature and the transition enthalpy of TBA salt hybrid PP55-T were very close to those of the corresponding polymer P55, which may indicate similar hydration of the polymer below TT in both cases. In contrast, the increase of the sharpness of the transition reveals a change in the transition mechanism likely due to a more rapid dehydration (transition in one step) as a consequence of the presence of hydrophobic TBA ions closely

associated to the POM head group in water. On the other hand, for the NH_4^+ hybrids PP55-N a significantly lower enthalpy per monomer was determined.

When NH_4^+ salt hybrids of different molar masses were studied, the change in shape (*i.e.* the broader transition), the decrease in enthalpy and the shift in the maximum of the transition temperature were most important for the hybrid possessing the shortest polymer chain (PP30-N), *i.e.* with the greatest proportion of POM. In the literature, such an increase of the transition temperature accompanied with a decrease in ΔH has been reported for thermoresponsive polymers with hydrophilic or charged moieties incorporated within the main chain. It has been proposed that incorporating hydrophilic or charged units increases the overall hydrophilicity of the polymer, and that the transition temperature is increased due to stronger interactions between the hydrophilic units and water.[37-39] Indeed, the transition enthalpy is related to the TT as H-bonds weaken with increased temperature.[37,38] A partial dehydration of thermoresponsive monomer units during the transition has also been considered in the presence of vicinal hydrophilic or charged monomers.[40] Similar to these studies, an increased overall hydrophilicity due to the presence of the hydrophilic ammonium-surrounded POM units might be a reason for the observed low ΔH values of our NH_4^+ hybrids.

Alternatively, a decrease in enthalpy has also been explained by interaction of polymer chains with surfaces, resulting in a limited hydration of the thermosensitive polymer at low temperature. For instance, it has been shown that adsorption of PNiPAAm on silica surfaces led to wider transitions with decreased ΔH.[19,41] Similar to these latter studies, one may assume that the observed smaller transition enthalpy for our NH_4^+ hybrids and the broader, more gradual phase transition is related to a reduced hydration of the PDEAAm at low temperature due to interactions with the POM surface. Given the much smaller surface and the compactness of POMs compared to the studied surfaces, and in view of DLS and cryo-TEM analyses that suggest an enhanced stabilization of the ammonium salt hybrids at 70°C (thanks to the charges provided by the hydrophilic POM) it seems reasonable to favor an explanation considering stronger interactions with water and poorer dehydration of the polymer.

These results demonstrate that the POM end-group and especially the nature of the counterion have an impact on the transition mechanism of PDEAAm: in the case of the TBA salt hybrid the transition enthalpy was similar to PDEAAm-C_{12}, whereas it was significantly lower in the case of the ammonium salt hybrids. The difference between the TBA and the NH_4^+ hybrids must be

attributed to the nature of the counterions. In contrast to NH_4^+, hydrophobic TBA ions are closely associated to the hydrophilic negatively charged POM surface in water, making the transition sharper and faster likely through a quickly occurring hydrophobic interchain aggregation.[42] In contrast to our former results obtained for POM-PDEAAm hybrid with a much shorter polymer chain (5000 g mol^{-1}), the transition temperature of the polymer and the hybrids are very close in the here-studied hybrids with rather long PDEAAm chains (30 to 90 kg mol^{-1}), most likely due to the small weight proportion of the POM unit.[11e]

DLS analyses and cryo-TEM shed light on the behavior of polymers and the corresponding hybrids in aqueous solution/dispersion. It was shown that PDEAAm-H (compound P55-H, without any hydrophobic dodecyl alkyl chain) was not simply molecularly dissolved in water at 20 °C, but that solvent-swollen poorly light-scattering aggregates exist in the PDEAAm samples (Figure SI-6). It was reported that such micro-gel-like swollen aggregates of PDEAAm in water are quite stable, exist even at low polymer concentration (also observed in this study) and are difficult to disaggregate.[43] However, when a dodecyl chain was added to PDEAAm, molecularly dissolved unimers were detected in solution (see number-derived size distribution in Figure SI-5), in addition to poorly light-scattering aggregates of various sizes. It seems thus that the introduction of a C_{12} alkyl chains, known to associate in aqueous media, has an impact on the conformational organization of the chains. The (diffuse) aggregates formed in the presence or absence of the dodecyl chain most likely do not possess the same organization, but at this stage and with the techniques available we are not able to give any further explanations. Still, the observed difference is in accordance with DSC results, revealing a slight change in the TT and ΔH. It should also be noted that micellization is often observed for alkyl-terminated semi-telechelic water-soluble polymers, but was not observed here for PDEAAm-C_{12}. This should be related to the relatively high molar mass of the polymer chains since it has been reported that alkyl end-capped thermoresponsive polymers of a molar mass beyond 30 kg mol^{-1} do not form micelles in aqueous media any more but are molecularly dissolved in water.[21b,44]

Similar to PDEAAm-C_{12} samples, DLS and cryo-TEM established that POM-polymer hybrids were dissolved as unimers in water at 20°C but the presence of loose aggregates was again demonstrated. The size of the unimers agrees with the estimation of the hydrodynamic radius of the hybrids in water for a gaussian polymer coil (Table SI-2). To compare these results with existing studies, one may compare the multiply-charged POM to a small polyelectrolyte block of

a diblock copolymer. For instance, PAA-*b*-PDEAAm diblock copolymers with a PDEAAm molar mass comparable to that of the POM-polymer conjugate and ω-end-capped by a hydrophobic C_{18} group have similar dimensions in water at pH 12 (diameter of about 10 nm). Similar to the present study, some larger aggregates were also detected.[27] At this pH the polyacrylic acid (PAA) segment may roughly mimic the charged POM unit, even though their respective conformations cannot be compared.[23,27]

Interestingly, for hybrid PP15-T possessing a very short polymer chain (M_n = 15 kg mol^{-1}), no unimers were detected by DLS (Figure SI-8) likely due to aggregation promoted by the important proportion of the hydrophobic α-TBA-POM and the ω-C_{12} chain end (Figure SI-8). When hybrid PP15-T or very high concentrated aqueous solutions of TBA salt hybrid PP55-T were analyzed by cryo-TEM (Figure 6b and Figure SI-9), an ordered organization was observed presumably based on the gathering of several hybrids driven by the assembly of the hydrophobic POM-TBA segments. This indicates again the importance of the TBA cation and the existence of a critical aggregation concentration (CAC) for the TBA hybrids at 20°C.

Table 5. Comparison of the polymers and hybrids at 70°C by DLS.

compound	***D*z range (nm)**	**Effect of wt%$_{POM}$ or $M_{nPDEAAm}$**	**Effect of solution concentration**	**Reversibility of the transition**
PDEAAm-H	10 - 200	n.a.	++ conc↑ => *PDI* ↑ & Dz↓↓	no
PDEAAm-C_{12}	~40	n.a.	+ conc↑ => *PDI* ↑↑ (& Dz↓)	yes
PPX-N	~40	-	-	yes
PPX-T	50-100	++ %POM↑/Mn↓ => Dz↑ (& *PDI* ↑)	++ conc↑ => Dz↑ & *PDI* ↑	yes

n.a. = not applicable; -, +, ++ de note no or poor effect, significant effect or strong effect.

Above the TT, the initial loose micro-gel-type aggregates of PDEAAm-H collapsed to form strongly light scattering aggregates (Figure SI-6, Table 4 and 5). Their diameter was concentration dependent. For sample PP55-H at 5 mg mL^{-1}, the aggregates' size was smaller than those of the initial microgels at 20°C, which might indicate their contraction. As reported before, a strong impact of the polymer concentration, heating duration and number of heating cycles on the diameter and aggregation number of the aggregates and their size distribution was observed.[18,22]

In contrast, in the presence of a dodecyl ω-chain end (PDEAAm-C_{12} samples) the initially present unimers aggregated to form bigger particles at 70°C. The aggregates size distribution increased strongly with increasing polymer concentration, but the average-diameter was only little affected. It remained in the range of 40 nm. The polymer length and the number of heating cycles did not significantly modify the diameters measured, indicating again that the system was reversible.

A clear impact of the POM units and especially the associated counterion was observed at 70°C when polymers and hybrids with PDEAAm of similar length were compared. Based on DLS results, aggregates of NH_4^+ hybrids had in general similar dimensions as those of PDEAAm-C_{12}. However, the size of the hybrids' aggregates was very reproducible and was affected neither by the concentration nor by the polymer chain length, whereas the former had an impact in the case of PDEAAm-C_{12} (and PDEAAm-H). The enhanced stabilization should be attributed to the additional electrostatic stabilization imparted by the hydrophilic charged POM unit. One can thus conclude that the ammonium salt hybrids form stable aggregates of rather constant aggregation number. Compared to PDEAAm-C_{12} and the NH_4 salt hybrids, the corresponding TBA salt hybrids formed larger aggregates at 70°C. Their size increased with the proportion of the POM content in the hybrids. In this case, the higher the weight percentage of the inorganic part (*i.e.* the smaller the molar mass of the PDEAAm chain), the larger were the aggregates. The observed changes in size can thus not be attributed to the variation in polymer length - as no effect of the M_n has been observed for PDEAAm-C_{12} - and can only be explained by the presence of the POM to which hydrophobic counterions are associated (Table 5). As discussed above, unlike the hydrophilic ammonium counterions, the TBA counterions are only poorly solvated in water and remain closely associated to the polyanionic POM surface, leading to a reorganization of the poorly stabilized aggregates, manifested by the larger aggregate size.

This influence of the POM unit wanes when the polymer chain becomes longer. Especially in the case of the smallest hybrid, PP15-T, a very large size distribution was observed indicating poor stabilization. For this hybrid possessing a PDEAAm chain of only about 10 kg mol^{-1}, not only the hydrophobic POM TBA part (at its α-end) contributes with 41 wt% to the hydrophobization of the compound, but also the hydrophobic C_{12} at the ω-end should now have an impact on the transition and drive the assembly of the compound at low temperature.[21] For all TBA salt hybrids, the size of the aggregates increased with concentration, certainly due to the increased proximity of the polymer chains when aggregation occurs.[18,22,34] The tendency of the POM-TBAs to aggregate and the existence of a CAC at 20°C was also observed by cryo-TEM analysis of PP15-T solutions and also for highly concentrated aqueous solutions of TBA salt hybrid PP55-T. This concentration-depended aggregation at both 20°C and 70°C highlights again the crucial role of the closely associated hydrophobic TBA counterion on the aggregation mechanism.

CONCLUSION

Similar to semitelechelic ω-dodecyl poly(*N*,*N*-diethylacrylamides), aqueous solutions of α_1-Dawson POM-PDEAAm hybrids are at 20°C constituted of unimers and microgel-type swollen aggregates. Upon heating both series undergo phase transition due to the rupture of hydrogen bonds, and nanometric aggregates (mesoglobules) form. For all compounds the transition started at around 30°C, but the maximum of the transition and its broadness was strongly influenced by the presence of the negatively-charged POM at the α-end of the polymer and the type of the counterions. In the presence of closely associated hydrophobic TBA counterions, the transition was sharper than for the other compounds, with an enthalpy close to that of the purely organic polymer. This indicates similar hydration of the polymer but a change in the aggregation mechanism. In contrast, for the hydrophilic NH_4^+ salt, the transition was prolonged and the enthalpy was smaller, showing again a change in the aggregation mechanisms presumably due to an enhanced stabilization provided by the negatively charged hydrophilic POM units.

DLS and cryo-TEM analyses were consistent with the DSC observations, and revealed an enhanced stability of the NH_4^+ hybrids provided by the charged POMs. Nanometer-sized aggregates (40-50 nm) were reproducibly formed, independently of the polymer concentration or the molar mass of the PDEAAm chain. Stable aggregates were also formed with TBA

counterions, but their size increased with the solution concentration and the proportion of the POM in the hybrid. The hydrophobic effect of the TBA salt was further revealed at 20°C by cryoTEM analyses. For highly concentrated solutions or hybrids possessing a short PDEAAm chain, i.e. a large proportion of POM, micellar aggregates were observed, whose formation is likely driven by hydrophobic interactions.

The conformation of POM-PDEAAm hybrids in water and their assembly into colloidally stable aggregates is thus tunable and may be triggered by external factors, such as the temperature and the nature of counterion or the concentration. These features bode well for further applications of the conjugates, especially in view of the catalytic activity of the inorganic clusters and the possibility to alter it reversibly in these smart materials.

Supporting Information available. The Supporting Information provides additional DSC thermograms, DLS plots, and cryo-TEM image. It also reports the mean diameters of aqueous solutions of polymers and hybrids at 20°C and the theoretical calculation of the radius of gyration.

Acknowledgement. The authors thank the Ile-de-France region for JLH's PhD grant. Jean-Michel Guigner and Patricia Beaunier are acknowledged for electron microscopy analyses, and Dominique Hourdet and Laurent Bouteiller for fruitful discussions.

References

[1] Song, Y.-F; Tsunashima, R. *Chem. Soc. Rev*. **2012**, *41*, 7384.
[2] Miras, H. N.; Yan, J.; Long, D.-L.; Cronin, L. *Chem. Soc. Rev*. **2012**, *41*, 7403.
[3] Themed issue: Polyoxometalate Cluster Science; *Chem. Soc. Rev*. **2012**, *41*, 7325.
[4] Hasenknopf, B. *Front. Biosci*. **2005**, *10*, 275.
[5] Dolbecq, A.; Dumas, E;. Mayer, C. R.; Mialane P. *Chem. Rev*., **2010**, *110*, 6009.
[6] Proust, A.; Matt, B.; Villanneau, R.; Guillemot, G.; Gouzerh, P.; Izzet, G. *Chem. Soc. Rev*., **2012**, *41*, 7605.
[7] Thorimbert, S.; Hasenknopf, B.; Lacôte, E. *Isr. J. Chem.*, **2011**, *51*, 275.
[8] Judeinstein, P. *Chem. Mater*. **1992,** 4, 4.
[9] a) Mayer, C. R.; Thouvenot, R.; Lalot, T. *Chem. Mater*. **2000**, *12*, 257-260; b) Moore, A. R.; Kwen, H.; Beatty, A. M.; Maatta, E. A. *Chem. Commun*. **2000**, 1793-1794; c) Xu, L.; Lu, M.; Xu, B.; Wei, Y.; Peng, Z.; Powell, D. R. *Angew. Chem., Int. Ed*. **2002**, *41*, 4129-4132; d) Lu, M.; Xie, B.; Kang, J.; Chen, F.-C.; Yang, Y.; Peng, Z. *Chem. Mater*. **2005**, *17*, 402-408.
[10] a) Qi, W.; Wu, L. *Polym. Int*. **2009**, *58*, 1217-1225; b) Song, Y.-F.; Tsunashima, R. *Chem. Soc. Rev*. **2012**, *41*, 7384.

[11] a) Han, Y.; Xiao, Y.; Zhang, Z.; Liu, B.; Zheng, P.; He, S.; Wang, W. *Macromolecules* **2009**, *42*, 6543; b) Han, Y.-K.; Zhang, Z.-J.; Wang, Y.-L.; Xia, N.; Liu, B.; Xiao, Y.; Jin, L.-X.; Zheng, P.; Wang, W. *Macromol. Chem. Phys.* **2011**, *212*, 81; c) Xiao, Y.; Han, Y.-K.; Xia, N.; Hu, M.-B.; Zheng, P.; Wang, W. *Chem. Eur. J.* **2012**, *18*, 11325; d) Xia, N.; Yu, W.; Wang, Y.; Han, Y.; Zheng, P.; Wang, W.; Sakaguchi, G.; Matsuda, K.; Saijo, K.; Takenaka, M.; Hasegawa, H. *Polymer* **2011,** *52*, 1772; e) Rieger, J.; Antoun, T.; Lee, S. H.; Chenal, M.; Pembouong, G.; Lesage de la Haye, J.; Azcarate, I.; Hasenknopf, B.; Lacôte, E. *Chem. Eur. J.* **2012**, *18*, 3355; f) Hu, M.-B.; Xia, N.; Yu, W.; Ma, C.; Tang, J.; Hou, Z.-Y.; Zheng, P.; Wang, W. *Polym. Chem.* **2012**, *3*, 617; g) Chakraborty, S.; Keightley, A.; Dusevich, V.; Wang, Y.; Peng, Z. *Chem. Mater.* **2010**, *22*, 3995; h) Chakraborty, S.; Jin, L.; Li, Y.; Liu, Y.; Dutta, T.; Zhu, D.-M.; Yan, X.; Keightley, A.; Peng, Z. *Eur. J. Inorg. Chem.* **2013**, 1799; i) Cannizzo, C.; Mayer, C. R.; Sécheresse, F.; Larpent, C. *Adv. Mater.* **2005**, *17*, 2888; j) Azcarate, I.; Ahmed, I.; Farha, R.; Goldmann, M.; Wang, X.; Xu, H.; Hasenknopf, B.; Lacôte, E.; Ruhlmann, L. *Dalton Trans.* **2013**, *42*, 12688; k) Xiao, Y.; Chen, D.; Ma, N.; Hou, Z.; Hu, M.; Wang, C.; Wang, W. *RSC Advances* **2013**, *3*, 21544; l) Miao, W.-K.; Yan, Y.-K.; Wang, X.-L.; Xiao, Y.; Ren, L.-J.; Zheng, P.; Wang, C.-H.; Ren, L.-X.; Wang, W. *ACS Macro Lett.* **2014**, *3*, 211; m) Hu, B.; Wang, C.; Wang, J.; Gao, J.; Wang, K.; Wu, J.; Zhang, G.; Cheng, W.; Venkateswarlu, B.; Wang, M.; Lee, P. S.; Zhang, Q., *Chem. Sci.* **2014**, 5, 3404; n) Lesage de La Haye, J.; Guigner, J.-M.; Marceau, E.; Ruhlmann, L.; Hasenknopf, B.; Lacôte, E.; Rieger, J. *Chem. Eur. J.* **2015**, *DOI: 10.1002/chem.201405708*.
[12] a) Chen, H.; Yang, Y.; Wang, Y.; Wu, L. *Chem. Eur. J.* **2013**, *19*, 11051; b) Wie, H.; Shi, N.; Zhang, J.; Guan, Y.; Zhang, J.; Wan, X. *Chem. Commun.***2014**, 50, 9333.
[13] Han, Y.; Xiao, Y.; Zhang, Z.; Liu, B.; Zheng, P.; He, S.; Wang, W., *Macromolecules* **2009,** *42*, 6543.
[14] Han, Y.-K.; Zhang, Z.-J.; Wang, Y.-L.; Xia, N.; Liu, B.; Xiao, Y.; Jin, L.-X.; Zheng, P.; Wang, W. *Macromol. Chem. Phys*. **2011**, *212*, 81.
[15] Tong, U.; Chen, W.; Ritchie, C.; Wang, X.; Song, Y.-F., *Chem. Eur. J.* **2014**, *20*, 1500.
[16] Lesage de la Haye, J.; Beaunier, P.; Ruhlmann, L.; Hasenknopf, B.; Lacôte, E.; Rieger, J. *ChemPlusChem* **2014**, *79*, 250.
[17] Uguzdogan, E.; Denkbas, E. B.; Kabasakal, O. S. *J. Appl. Polym. Sci.*, **2013**, *127*, 4374.
[18] Shen, L.; Zhang, G-Z. *Chin. J. Polym. Sci.* **2009**, *27*, 561.
[19] Schönhoff, M.; Larsson, A.; Welzel, P. B.; Kuckling, D., *J. Phys. Chem. B* **2002,** *106*, 7800.
[20] Chung, J. E.; Yokoyama, M.; Aoyagi, T.; Sakurai, Y.; Okano, T. *J. Control. Release* **1998**, *53*, 119.
[21] a) Kujawa, P.; Segui, F.; Shaban, S.; Diab, C.; Okada, Y.; Tanaka, F.; Winnik, F. *Macromolecules* **2006**, *39*, 341; b) Obeid, R.; Tanaka, F.; Winnik, F. *Macromolecules* **2009**, *42*, 5818.
[22] Lu, Y.; Zhou, K.; Ding, Y.; Zhang, G.; Wu, C., *Phys. Chem. Chem. Phys.* **2010,** *12*, 3188.
[23] Delaittre, G.; Save, M.; Gaborieau, M.; Castignolles, P.; Rieger, J.; Charleux, B. *Polym. Chem.* **2012**, *3*, 1526.
[24] Gan, L. H.; Cai, W.; Tam, K. C., *Eur. Polym. J.* **2001,** *37*, 1773.
[25] Shechter, I.; Ramon, O.; Portnaya, I.; Paz, Y.; Livney, Y. D. *Macromolecules*, **2010**, *43*, 480.
[26] Paz, Y.; Kesselman, E.; Fahoum, L.; Portnaya, I.; Ramon, O. *J. Polym. Sci*., *Part B : Polym Phys*. **2004**, *42*, 33.
[27] André, X.; Zhang, M.; Müller, A. H. E. *Macromol. Rapid Commun*. **2005**, *26*, 558.
[28] Trinh, L. T. T.; Lambermont-Thijs, H. M. L.; Schubert, U. S.; Hoogenboom, R.; Kjøniksen, A.-L. *Macromolecules* **2012**, *45*, 4337.
[29] a) Etika, K. C.; Jochum, F. D.; Theato, P.; Grunlan, J. C. *J. Am. Chem. Soc*. **2009**, *131*, 13598; b) Etika, K. C.; Jochum, F. D.; Cox, M. A.; Schattling, P.; Theato, P.; Grunlan, J. C. *Macromol. Rapid Commun.* **2010**, *31*, 1368.
[30] Fujishige, S.; Kubota, K.; Ando, I. *J. Phys. Chem*. **1989**, *93*, 3311.
[31] Boutris, C.; Chatzi, E. G.; Kiparissides, C. *Polymer* **1997**, *38*, 2567.
[32] Idziak, I.; Avoce, D.; Lessard, D.; Gravel, D.; Zhu, X. X. *Macromolecules* **1999,** *32*, 1260.
[33] Maeda, Y.; Yamabe, M. *Polymer* **2009**, 50, 519.
[34] Aseyev, V.; Tenhu, H.; Winnik, F. M. *Adv. Polym. Sci*. **2011**, *242*, 29.
[35] Maeda, Y.; Nakamura, T. Ikeda, I. *Macromolecules* **2002**, *35*, 10172.
[36] Lessard, D. G.; Ousalem, M.; Zhu, X. X. *Can. J. Chem*. **2001**, *79*, 1870.
[37] a) Feil, H.; Bae, Y. H.; Feijen, J.; Kim, S. W. *Macromolecules* **1993**, *26*, 2496; b) Kuckling, D.; Adler, H.-J.; Arndt, K.- F.; Ling, L.; Habicher, W. D. *Macromol. Symp.* **1999**, *145*, 65.
[38] Maeda, Y.; Yamamoto, H.; Ikeda, I. *Langmuir* **2001**, *17*, 6855.
[39] Maeda, Y.; Yamamoto, H.; Ikeda, I. *Colloid Polym. Sci*. **2004**, *282*, 1268.
[40] Siband, E.; Tran, Y.; Hourdet, D. *Macromolecules* **2011**, *44*, 8185.
[41] Petit, L.; Bouteiller, L.; Brûlet, A.; Lafuma, F.; Hourdet, D. *Langmuir* **2007**, *23*, 147.

[42] Chaumont, A.; Wipff, G. *Phys. Chem. Chem. Phys*. **2008**, *10*, 6940.
[43] Itakura, M.; Inomata, K.; Nose, T., *Polymer* **2000,** *41*, 8681.
[44] Obeid, R.; Maltseva, E.; Thünemann, A. F.; Tanaka, F.; Winnik, F. M. *Macromolecules* **2009**, *42*, 2204.

Supporting Information

Study of the temperature-induced aggregation of polyoxometalate-poly(*N*,*N*-diethylacrylamide) hybrids in water

Jennifer Lesage de la Haye,[a,b,c] André Pontes da Costa,[a,b] Gaëlle Pembouong,[a,b] Laurent Ruhlmann,[d] Bernold Hasenknopf,*[a,b] Emmanuel Lacôte,*[c,e] Jutta Rieger*[a,b]

[a] Sorbonne Universités, UPMC Univ Paris 06, UMR 8232, Institut Parisien de Chimie Moléculaire (IPCM), F-75005, Paris, France.

[b] CNRS, UMR 8232, Institut Parisien de Chimie Moléculaire (IPCM), F-75005, Paris, France.

[c] ICSN CNRS, Av. de la Terrasse, 91198 Gif-sur-Yvette Cedex, France.

[d] Université de Strasbourg, Laboratoire d'Electrochimie et de Chimie Physique du Corps Solide, Institut de Chimie, 67081 Strasbourg, France.

[e] Université de Lyon, Institut de chimie de Lyon, UMR 5265 CNRS-Université Lyon I-ESCPE Lyon, 69616 Villeurbanne, France.

*Corresponding Authors:

bernold.hasenknopf@upmc.fr, emmanuel.lacote@univ-lyon1.fr, jutta.rieger@upmc.fr

DSC measurements

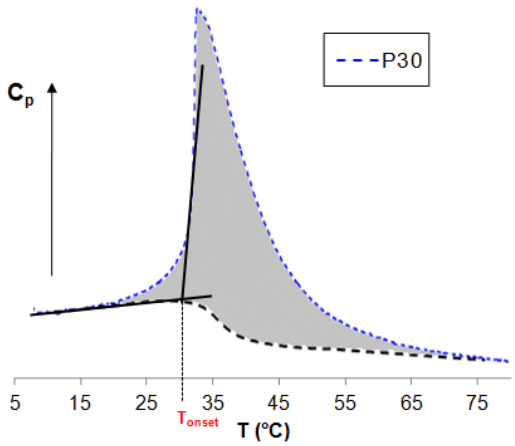

Figure SI-1. Treatment of the data of heat transfer measured by nanoDSC on an aqueous solution of P30 (5 mg mL^{-1}).

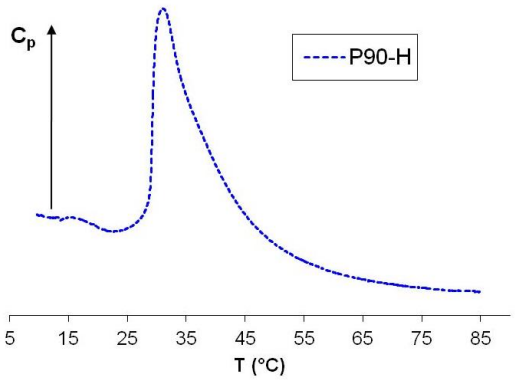

Figure SI-2. Temperature dependence of specific heat capacity (Cp in kJ mol_{DEAAm}^{-1} K^{-1}) of an aqueous solution of PDEAAm-H P90-H (5 mg mL^{-1}). Heating/cooling rates were 0.5 °C min^{-1}.

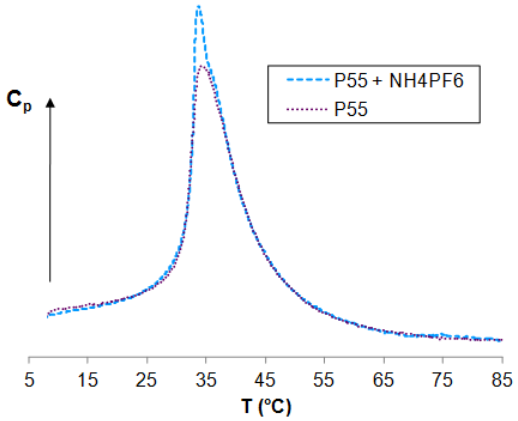

Figure SI-3. Temperature dependence of specific heat capacity (Cp in kJ mol_{DEAAm}^{-1} K^{-1}) of PDEAAm aqueous solutions (5 mg mL^{-1}) with and without NH_4PF_6 salts. Heating rates were 0.5 °C min^{-1}.

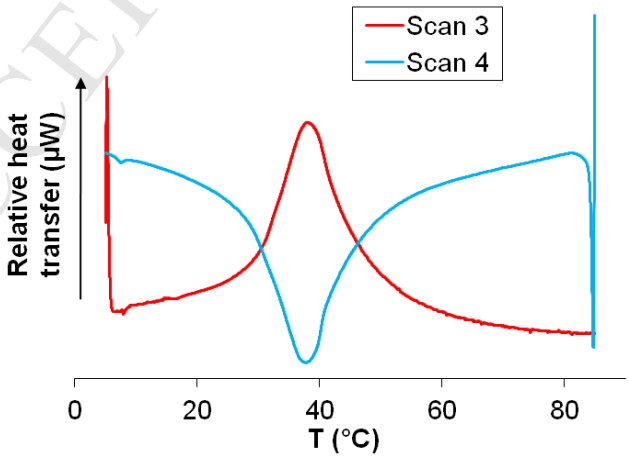

Figure SI-4. Endothermic heating scan (scan 3) and exothermic cooling scan (scan 4) of the aqueous solution (5 mg mL^{-1}) of PP55-N. Heating rates were 0.5 °C min^{-1}.

DLS measurements

PDEAAm-C_{12}

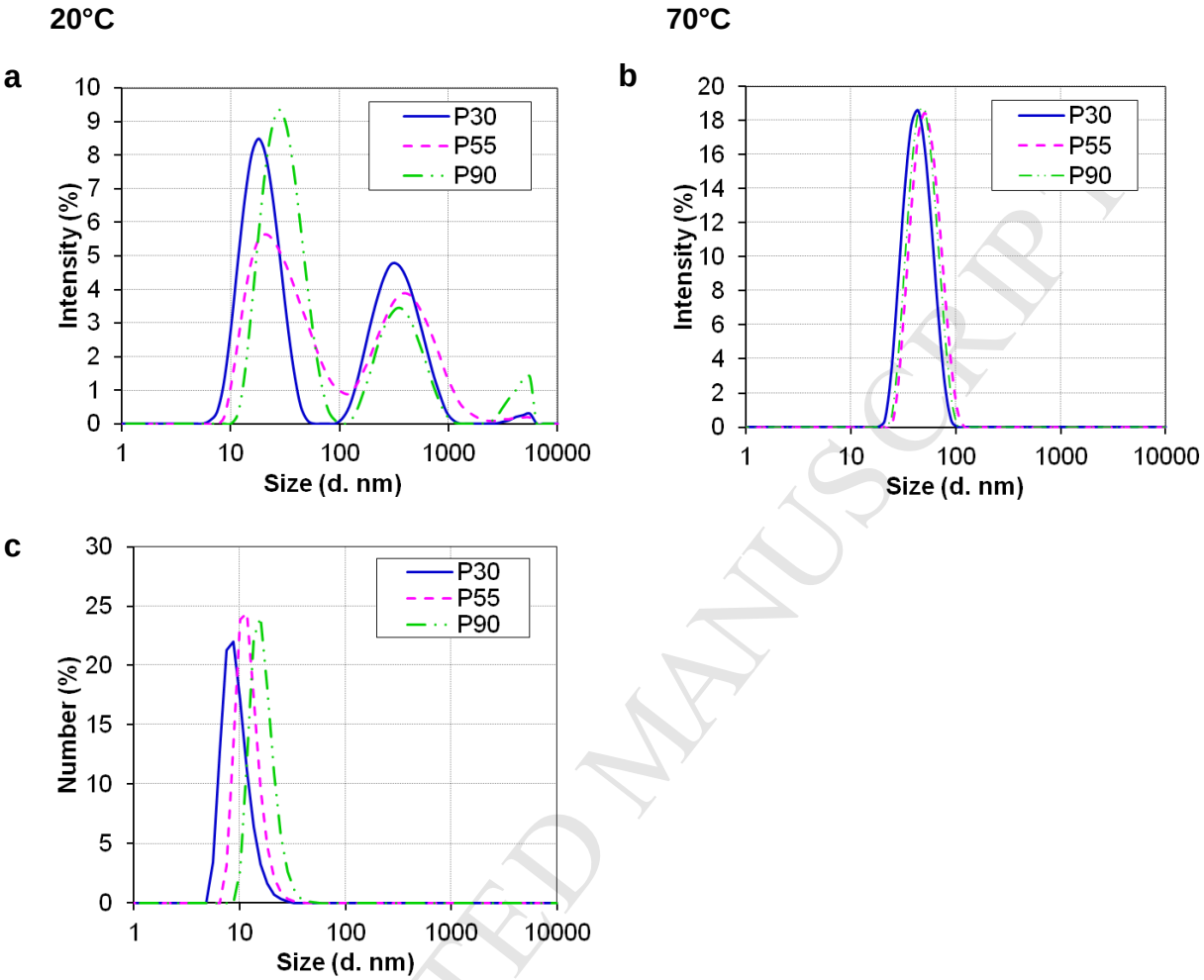

Figure SI-5. DLS data for solutions of PDEAAm-C_{12} (5 mg mL^{-1}) showing the intensity *vs* particle size (in diameter) plots at (a) 20 °C and (b) 70 °C and the number *vs* particle size (in diameter) plots at (c) 20 °C.

PDEAAm-H

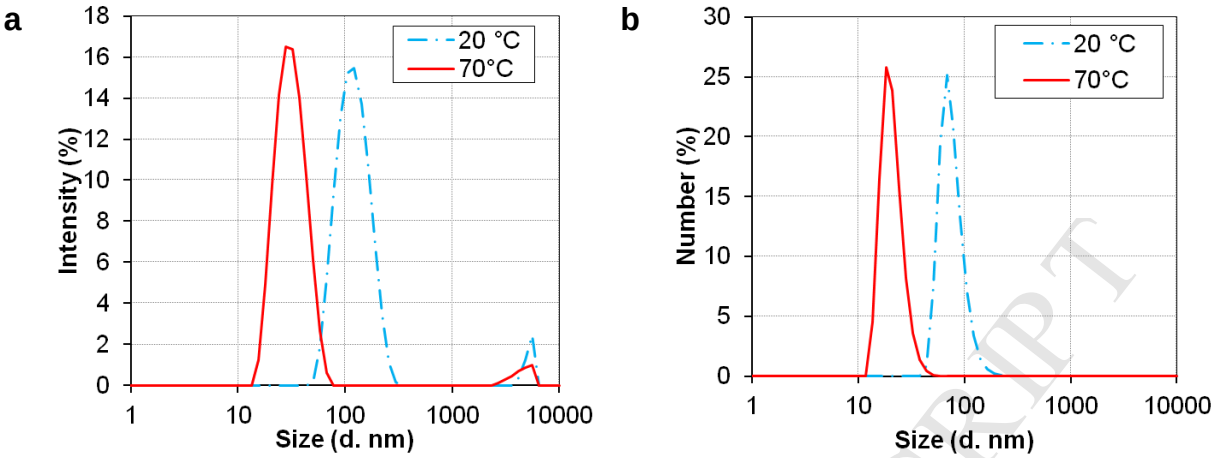

Figure SI-6. DLS data for solutions of PDEAAm P55-H (5 mg mL^{-1}) showing (a) the scattered intensity and (b) number *vs* particle size (in diameter) plots at 20 °C and 70 °C.

POM-polymer Hybrids

At 20°C

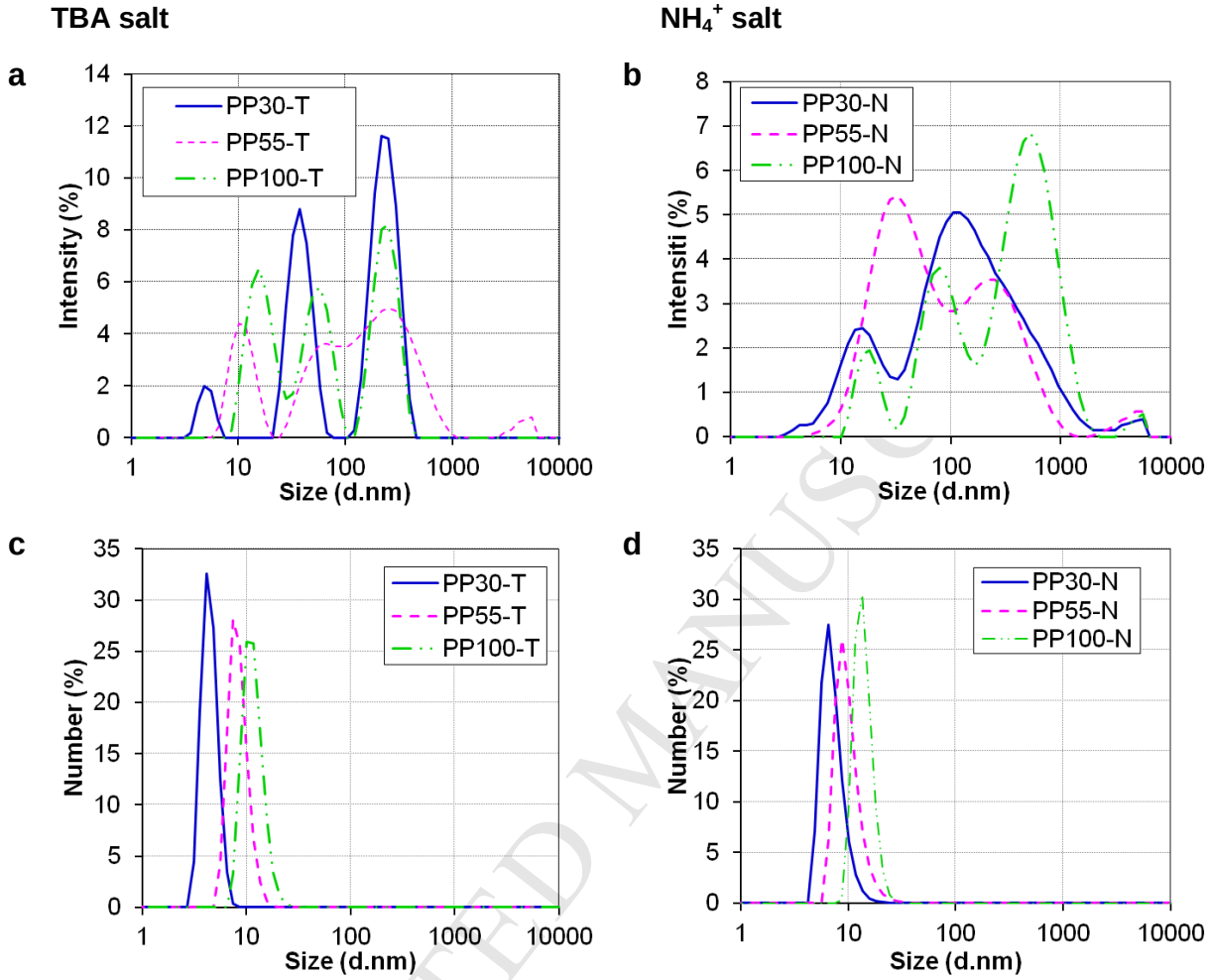

Figure SI-7. DLS data at 20 °C for solutions (5 mg mL^{-1}) of POM-PDEAAm hybrids showing the intensity *vs* particle size (in diameter) plots in (a) TBA salt and (b) NH_4 salt and the number *vs* particle size (in diameter) plots in (c) TBA salt and (d) NH_4^+ salt.

PP15-T

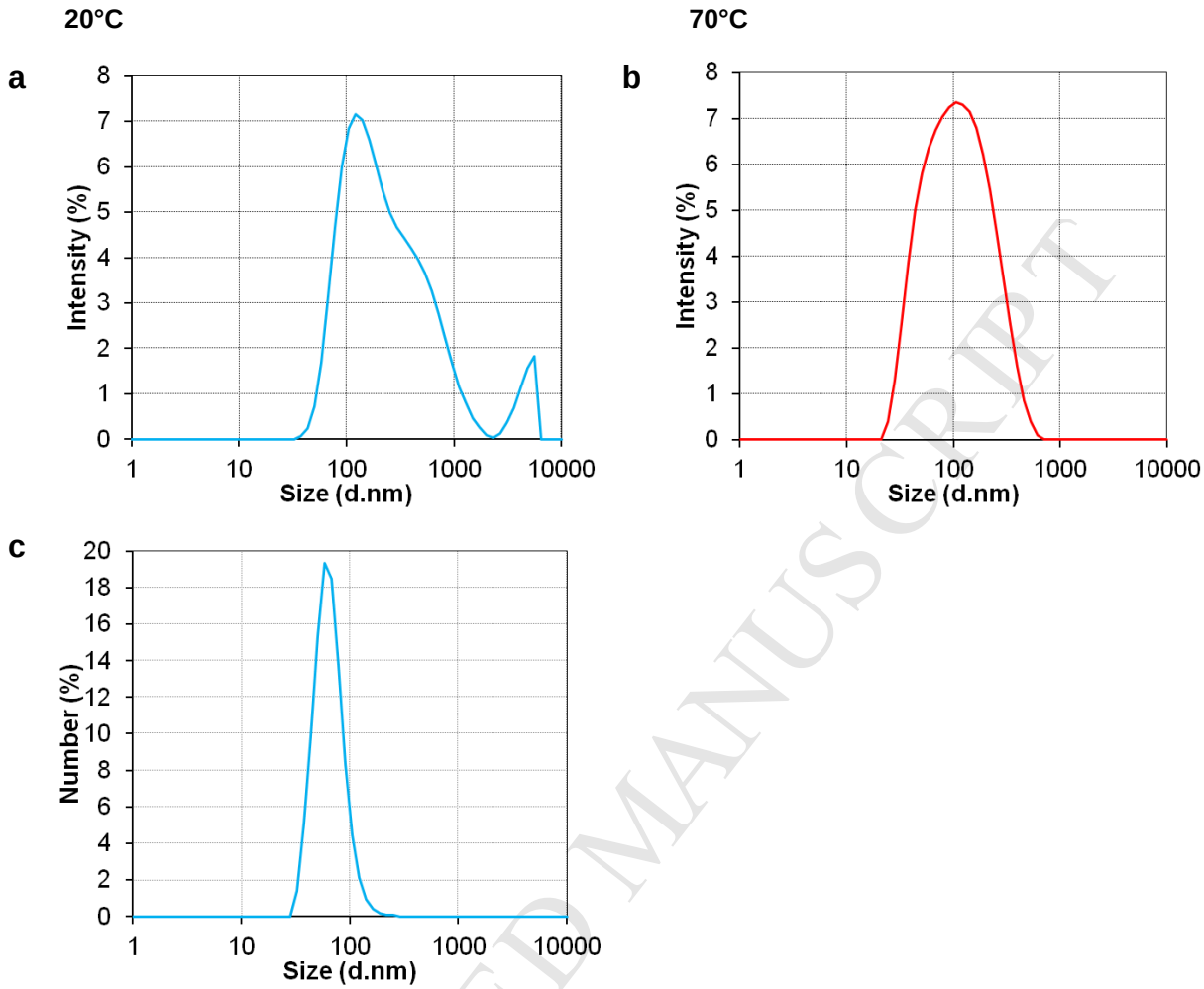

Figure SI-8. DLS data at (a) and (c) 20 °C and at (b) 70°C for solutions (5 mg mL^{-1}) of POM-PDEAAm PP15-T.

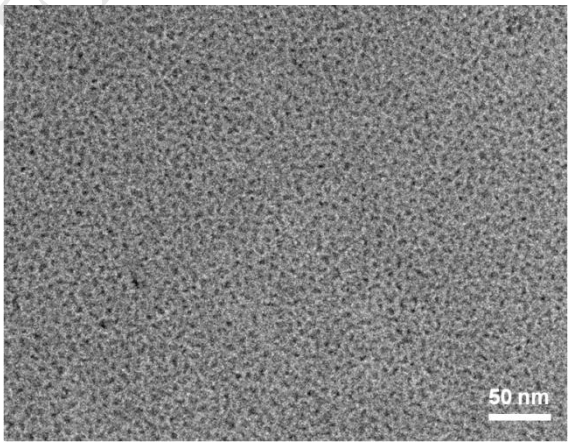

Figure SI-9. Cryo-TEM images of an aqueous solution of PP15-T fast-frozen from 20 °C at 5 mg mL^{-1}.

Table SI-1. Number mean diameter of unimers formed in aqueous solutions (5 mg mL^{-1}) of PDEAAm-C_{12}, PDEAAm-H and POM-polymer hybrids (TBA and NH_4^+ salts) at 20 °C.

number mean diameter (D_n, nm)									
PDEAAm-C_{12}			PDEAAm-H	POM-PDEAAm (NH_4^+ salt)			POM-PDEAAm (TBA salt)		
P30	P55	P90	P55-H	PP30-N	PP55-N	PP100-N	PP30-T	PP55-T	PP100-T
9	12	17	77	7	10	14	4	8	12

Table SI-2. Theoretical values for R_g and R_h of POM-polymer hybrids at 20 °C.

Entry[a]	DP_n[b]	R_g[c] / nm	R_h[d] / nm	R_n[e] (DLS) / nm
PP30	191	4.2	3.2	3.5
PP55	390	6.0	4.6	5.0
PP100	718	8.1	6.2	7.0

[a] « PP30 » stands for POM-polymer with $M_n \approx 30$ kg mol^{-1}.

[b] Number-average degree of polymerization calculated by $DP_n = [M_{n,LS}(PPXX) - MW(POM\text{-}TTC)]/MW(DEAAm)$

[c] Radius of gyration calculated using: $R_g = \sqrt{\frac{N.a^2.C_\infty}{6}}$ where N is the number of bond segment ($N = 2 \times DP_n$), a the length of each segment ($a = 0.154$ nm) and, and C_∞ the characteristic ratio of the polymer in the solvent used (water) ($C_\infty = 11.7$ for poly(*N*-isopropylacrylamide) in water).[1]

[d] Hydrodynamic radius determined from $R_g/R_h = 1.3$ for a linear polymeric chain in a theta solvent.[2]

[e] Hydrodynamic radius estimated by DLS for NH_4^+ salts hybrids (Table SI-1).

References

[1] Trongsatitkul, T. ; Budhlall, B. M.; *Polym. Chem*. **2013**, *4*, 1502-1517.

[2] *Polymer Physics* (p. 347); Rubinstein, M.; Colby, R. H., Ed.; Oxford University Press: Oxford, 2003.